Progress In Electromagnetics Research M, Vol. 64, 77–86, 2018

Statistical Modeling of Low-Latitude Long-Distance HF Ionospheric Multi-Mode Channels

Indah Kurniawati[1, 3, *], Gamantyo Hendrantoro[1], Wirawan[1], and Muhammad Taufik[2]

Abstract—Studies have been reported in the literature on High Frequency (HF) radio channels in mid-latitude areas more frequently than in low latitudes, where the ionospheric channels might behave differently. This paper reports a statistical model of HF sky wave channel complex impulse response and its parameters, i.e., channel gain, path gain, phase shift, and delay spread statistics, derived from both simulation and measurement on a 3044 km link in Indonesia. Evaluations show that multipaths observed with respect to their propagation delays form multiple clusters corresponding to different propagation modes. The channel gain is found to be Rayleigh distributed, whereas the rms and maximum delay spread exhibit Rayleigh and Gaussian distributions, respectively. This model can be used in performance evaluation of digital communication schemes in low-latitude HF channels.

1. INTRODUCTION

High frequency (HF) sky wave communication systems in 3–30 MHz band were the core of long distance communication systems in the past before the development of satellite technology. However, HF systems have recently gained renewed interest for emergency communications or low-rate remote monitoring in isolated or disaster-struck areas unreachable by other means which require infrastructures that are either undeployed or damaged.

HF sky wave systems exploit ionospheric layer at a height between 50–500 km as its propagation medium that refracts and reflects HF waves back to earth [1]. The diurnal and seasonal variations of free electron conditions, solar activities, geomagnetic position, and height of ionospheric layers greatly impact communication in HF sky wave channels [2]. Consequently, the channels are commonly time-varying and frequency-selective with limited bandwidth. Hence, the knowledge on characteristics of HF channel impulse response is crucial in designing an HF digital radio communication system.

Many existing channel models commonly refer to the Watterson model [3]. However, it is only valid for narrow band and excludes multipath components originating from multiple modes. A more accurate wideband modeling has been reported in [4], with validation against measurement over 800 kHz bandwidth on a 2070 km link [5, 6]. Nevertheless, this model is complicated because it consists many factors gained from ionosonde measurement that is not always available everywhere [7]. Channel impulse response measurements for longer distance (more than 3000 km) have also been reported in [4–6], all of which were made in mid-latitude regions. Ionosphere in low latitude geomagnetic regions is distinct from that in mid latitudes, e.g., the presence of fountain effect called equatorial anomaly [2]. To our knowledge, there have been only a few attempts to model the HF sky wave channel impulse response in low-latitude regions compared to the more explored mid- and high-latitudes. A study on HF channel in

Received 16 October 2017, Accepted 18 January 2018, Scheduled 30 January 2018
* Corresponding author: Indah Kurniawati (kurniawati12@mhs.ee.its.ac.id).
[1] Department of Electrical Engineering, Institut Teknologi Sepuluh Nopember, Indonesia. [2] Department of Geomatic Engineering, Institut Teknologi Sepuluh Nopember, Indonesia. [3] Department of Electrical Engineering, Muhammadiyah University, Surabaya, Indonesia.

low-latitude region (Thailand) with a 600 km link has been reported in [8], but the distance is considered short, in which a single 1F propagation mode is usually relied on.

In this paper, our original contribution is a low-latitude HF long distance channel impulse response model, which consists of multiple paths that might originate from different propagation modes. The statistics of channel parameters, i.e., channel gain, path gain, phase shift and delay spread, are derived from ray tracing-based simulation and real measurement on a 3044 km link in Indonesia. Our results indicate that in addition to channel gain, path gain, phase shift and delay, impulse response is also characterized by elevation angle of the propagation paths. The findings also suggest that channel gain follows Rayleigh distribution, whereas rms and maximum delay spread follow Rayleigh and Gaussian, respectively.

In Section 2 we start with mathematical expression of channel impulse response, the hypothesized statistical model, and evaluation methods that comprise simulation and measurement. Results on statistical channel parameters are presented in Sections 3 and 4, followed by discussions and conclusions in Section 5.

2. HF SKY WAVE CHANNEL MODELING

2.1. Mathematical Model

The impulse response of lowpass-equivalent HF sky wave channel can be formulated as:

$$h(\tau,\varepsilon) = \sum_n \alpha_n e^{-j\theta_n} \delta\left[\tau - \tau_n\right] \cdot \delta\left[\varepsilon - \varepsilon_n\right] \tag{1}$$

where α_n, θ_n, τ_n and ε_n represent gain, phase shift, delay and elevation angle of the n-th path. Channel gain S results from:

$$h(\tau,\varepsilon) = S \sum_n a_n(t) e^{-j\theta_k} \delta\left[\tau - \tau_k\right] \cdot \delta\left[\varepsilon - \varepsilon_n\right] \tag{2}$$

where $\sum\limits_n |a_n|^2 = 1$, so that

$$S = \sqrt{\sum_n |\alpha_n|^2}. \tag{3}$$

Power delay profile (PDP) of the channel is given by:

$$p(\tau,\varepsilon) = S^2 \sum_n |a_n|^2 \ \delta\left[\tau - \tau_n\right] \cdot \delta\left[\varepsilon - \varepsilon_n\right] \tag{4}$$

The root mean square (rms) delay spread can be obtained [9]:

$$\sigma_\tau = \sqrt{\overline{\tau^2} - (\bar{\tau})^2} \tag{5}$$

where $\bar{\tau}$ represents mean excess delay, expressed as:

$$\bar{\tau} = \frac{\sum\limits_k p\ (\tau_k) \cdot \tau_k}{\sum\limits_k p\,(\tau_k)} \tag{6}$$

and τ_k denotes delay time of the k-th path relative to the first path.

The second moment of mean excess delay is expressed as:

$$\overline{\tau^2} = \frac{\sum\limits_k p\,(\tau_k) \cdot \tau_k^2}{\sum\limits_k p\,(\tau_k)} \tag{7}$$

The maximum excess delay is expressed as $\tau_x - \tau_o$, with τ_x representing maximum delay, i.e., delay of the last path and τ_o delay of the first arriving path.

2.2. Statistical Hypotheses of Channel Parameters

2.2.1. Channel Gain

Channel gain S in Eq. (3) refers to the square root of total signal power received on each path with 1 watt transmit power. Different paths undergo different trajectories with different path gains. The difference in phase shift among different paths might vary widely when we consider wavelengths in the order of 30–100 meters, which is very small compared to total path length. This can be true for paths experiencing the same propagation mode and having only slightly different trajectories, and even more so for paths belonging to different propagation modes. Accordingly, we could safely assume that these paths are not correlated with one another. This reasoning leads to a hypothesis that the channel gain in Eq. (3) tends to have Rayleigh distribution.

2.2.2. Normalized Path Gain and Path Phase Shift

Normalized path gain a_n for the n-th path is obtained by dividing the path gain α_n by channel gain S, which makes it difficult to model a_n statistically. On the other hand, path phase shift is obtained from remainder of the division of path length by the wavelength, assuming that there is no additional phase shift caused by other mechanisms. Since path length can take any value depending on ionospheric condition, propagation mode and elevation angle, it is reasonable to hypothesize that the resulting phase is random and follows uniform distribution in $[0, 2\pi)$.

2.2.3. Delay Spread

Delay spread is a measure of channel time dispersion that approximates inverse of the channel coherence bandwidth representing maximum symbol rate that can be transmitted through the channel without equalization [9]. Path length variation may be caused by variety of modes in a channel and results in varying path arrival time. It is hence natural to surmise that the delay spread of a channel containing a single mode is shorter than that with multiple modes.

In Eq. (5) rms delay spread is computed based on mean excess delay, which in turn depends on delay and gain of each path. Since the gains of paths with different delays are not correlated with each other, it can be conjectured that rms delay spreads of impulse responses with a single mode have Rayleigh distribution.

Furthermore, time delay of each propagation path through the ionosphere can be described as random and normally distributed [10]. It implies that maximum excess delay, which is the interval between arrivals of the first and the last path in an impulse response, is also normally distributed.

2.2.4. Elevation Angle

The elevation angle of a path might indicate its propagation mode. Therefore, knowledge on elevation angle statistics is useful in finding a strategy to limit the arriving modes by choosing a receiving antenna with appropriate elevation pattern, thereby reducing the delay spread.

2.3. Simulation Method

The HF radio channel simulation is carried out by ray tracing using PropLab [11]. PropLab adopts the 2007 International Reference Ionosphere (IRI) model for the condition of ionospheric layers, which is adjusted to approximate the real condition by manually defining the 12-month mean sunspot number (SSN) and the effective SSN (IG index) [12].

SSN data are obtained from space weather radar (SWR) in Australia [13]. The geomagnetic A-index value is given by radio station WWV and WWVH [11]. The Appleton-Hartree model is adopted for ray tracing [14]. The method accommodates effects of earth magnetic field and collision between electrons and neutral particles. The dipole field model is selected for magnetic field with two exponential terms as collision frequency model.

Carrier frequency of 14 MHz is used, which has the longest period of being under MUF for the selected days. The geographical and geomagnetic locations of transmitter and receiver in Surabaya and

Merauke in Indonesia, respectively, are presented in Table 1. Ray tracing is carried out for May 11 and September 11, 2015, each with one hour intervals for 24 hours, resulting in 24 impulse responses in each day. From the total of 48 impulse responses, nine samples are excluded because none of the simulated paths arrive sufficiently close to the receiver location. The type of antenna used in this simulation is horizontal dipole with 93.89° transmit beam azimuth and 50 Watt transmit power.

Table 1. Geographical and geomagnetical coordinates of the transmitter and receiver.

Location	Geographical Coordinate	Geomagnetical Coordinate
Transmitter	7.28 S, 112.80 E	16.86 S, 174.43 E
Receiver	8.53 S, 140.42 E	16.52 S, 145.79 E

The transmit elevation angle used in ray tracing ranges from 10° to 50° with 0.1° steps because elevation angles smaller than 10° are almost impossible to occur in real measurement due to ground clutter. The azimuth angle is in the ±2° range around 93.89°, i.e., the transmitter-receiver bearing angle. The great circle distance equation [15] is used to measure the distance between the end of path on earth and the receiver to determine whether the path can be regarded as 'arriving' at the receiver.

2.4. Measurement

A measurement campaign is performed to measure the HF radio channel low pass-equivalent impulse responses. The measurement system block diagram and parameters have been reported in a previous paper [16], with the only change being the carrier frequency used herein, which is 14 MHz, instead of 7 MHz [17].

The locations of the transmitter and receiver are shown on the map in Figure 1. The transmitter is installed on top of Building B of the Institut Teknologi Sepuluh Nopember in Surabaya, while the receiver is on the rooftop of the Electrical Engineering Laboratory building, Musamus University, Merauke. The two sides are located in different time zones: the transmitter is in the Western Indonesia Standard Time zone (GMT +7) and the receiver in the Eastern Indonesia Standard Time zone (GMT +9). Meanwhile,

Figure 1. Transmitter and receiver locations in Surabaya and Merauke.

the wave bending in the ionosphere is considered to occur mostly in the Central Indonesia Standard Time zone (GMT +8). We subsequently refer to GMT +7 as local time (LT).

The measurement is carried out on February 12–15, 2014 in the hours when in western, central and eastern part of Indonesia it is successively sunrise (03:00–05:00 LT), noon (10:00–12:00 LT), sunset (16:00–18:00 LT), and night (19:00–23:00 LT). The total of measurement sessions is 20. We use 12th-order PN sequence resulting in a total of 4095 bits with 500 kbps bit rate and 1 MHz sampling. Hence, the total number of samples of PN sequence is 8190, so that the maximum measurable excess delay is 8.19 ms. In each session, multiple periods of PN sequence are transmitted for 5 seconds, resulting in a total of 561 periods or 2297295 samples. Weakness of the measurement system is relatively low resolution due to limited bandwidth, prohibiting separation of paths belonging in the same cluster.

An impulse response estimate is obtained by cross-correlating the original PN-sequence and the received IQ sequence. Noise filtering is applied to eliminate noise using the algorithm proposed by Sousa et al. [18]. The noise threshold is defined to obtain a constant false alarm rate (CFAR) by taking 5% probability of noise rising above the threshold. CFAR is applied to each PN correlation result, so that ten impulse responses are generated from the original ten periods, from which a time-averaged PDP is obtained.

3. RESULTS

3.1. Channel Gain and Phase Shift

Channel gain S is acquired from simulation results using Eq. (3) and analyzed further through its cumulative distribution function (CDF). The Kolmogorov-Smirnov (K-S) fitting test shows that the closest theoretical distribution fit to channel gain is Rayleigh as shown in Figure 2, which confirms the hypothesis in Section 2.

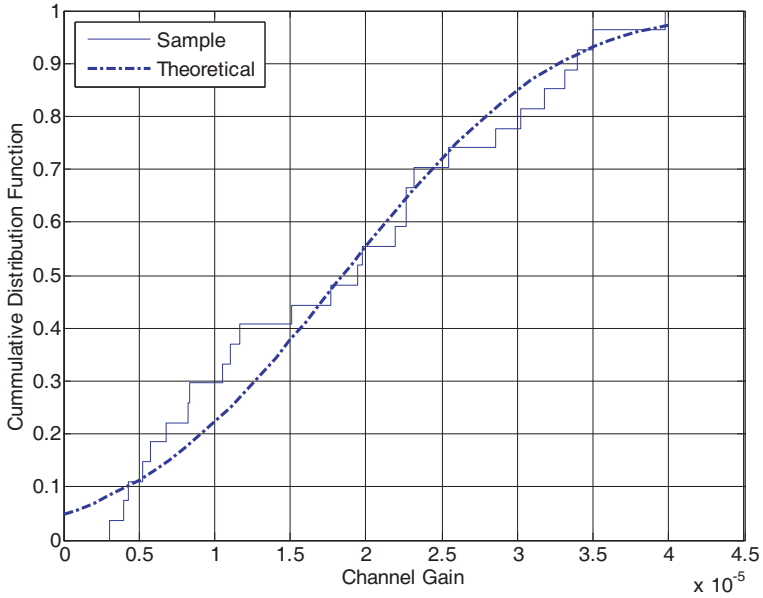

Figure 2. Cumulative distribution function of channel gain from ray tracing result.

Calculation of the path phase shift has been explained in Section 2.1. The K-S test of the CDF suggests that the nearest theoretical fit to this is the uniform distribution, in line with our conjecture in Section 2. Figure 3 shows visually the closeness of CDF of the path phase shift to the uniform distribution.

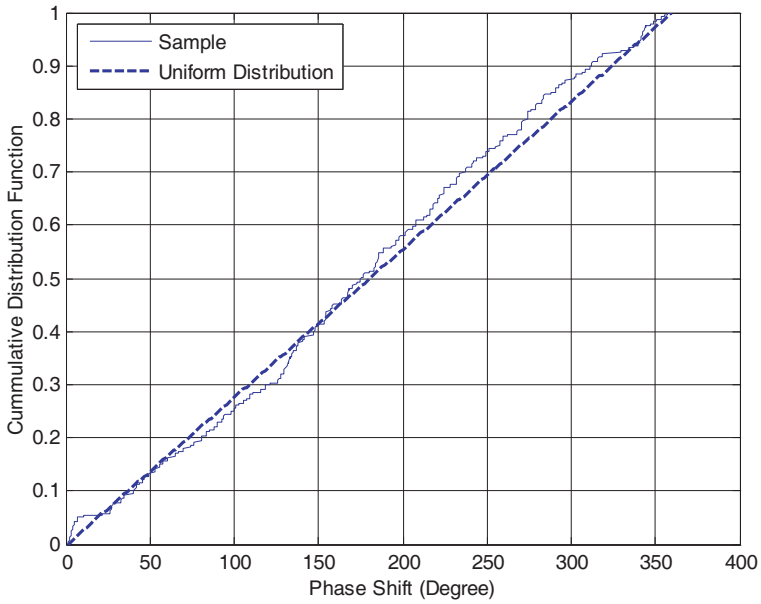

Figure 3. Cumulative distribution function of path phase shift of the ray tracing result.

3.2. Delay Spread

Invoking discrete-time impulse response model [19], the delay axis is divided into intervals called 'bin'. For each simulated channel, each bin might consist of a number of multipath components of different propagation modes.

The results of data processing suggest that it is best to divide the delay axis into three bins, 0–100 μs, 100–500 μs, and 500–1300 μs. This is done by taking into account all possible events of an impulse response having only a single mode, two simultaneous modes, or more. Table 2 recapitulates the binning results.

Table 2. Propagation modes occurrence in each excess delay bin.

Excess delay bin (ms)	2F		3F		4F	
	Total	Elevation angle (°)	Total	Elevation angle (°)	Total	Elevation angle (°)
0–100	56	12.8–21	99	19.8–30.4	-	-
100–500	21	12.6–20.8	28	19.7–30.1	-	-
500–1300	-	-	42	25.4–27.1	5	41.1–41.5

Figures 4 and 5 present path magnitude variation with respect to elevation angle and time delay for all simulated paths regardless of the bin they belong to. Figure 4 shows that the most dominant magnitude originates from paths with 2F propagation mode, which have smaller elevation angle than those from 3F and 4F. The paths in 4F mode are the least dominant in magnitude due to their highest elevation angles. Figure 5 shows that the paths can be classified into three clusters. The first cluster contains paths with the most dominant magnitudes arriving through 2F and 3F modes. The second cluster contains paths in 3F mode, and the third contains paths in 3F and 4F modes.

Figures 6 and 7 present CDFs of rms delay spread as the results of ray tracing simulation and field measurement, respectively, plotted together with the theoretical Rayleigh CDF with the same statistical parameters. Visual inspection and K-S test suggest that Rayleigh distribution provides a good fit to rms delay spread obtained from ray tracing and field measurement [20]. This is in line with our hypothesis in Section 2.

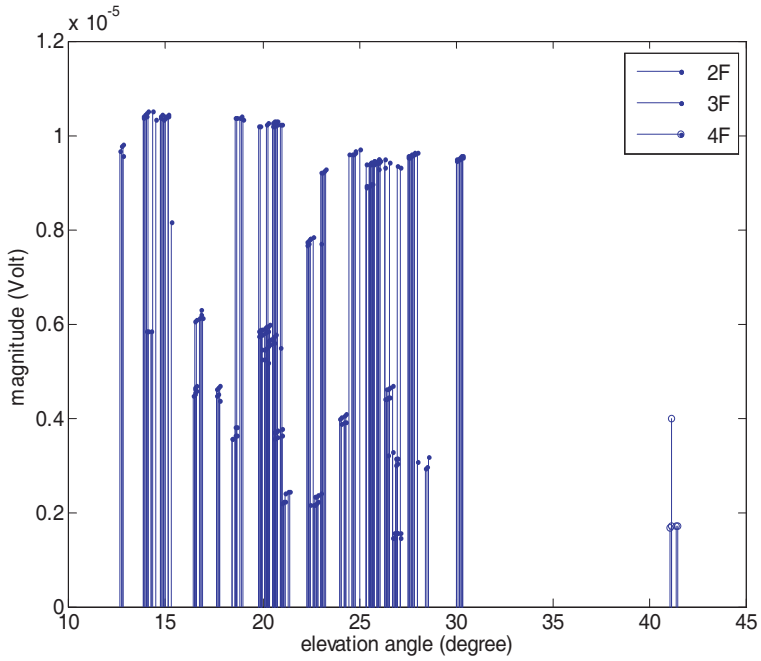

Figure 4. Received signal magnitudes with respect to elevation angles for all of paths from ray tracing.

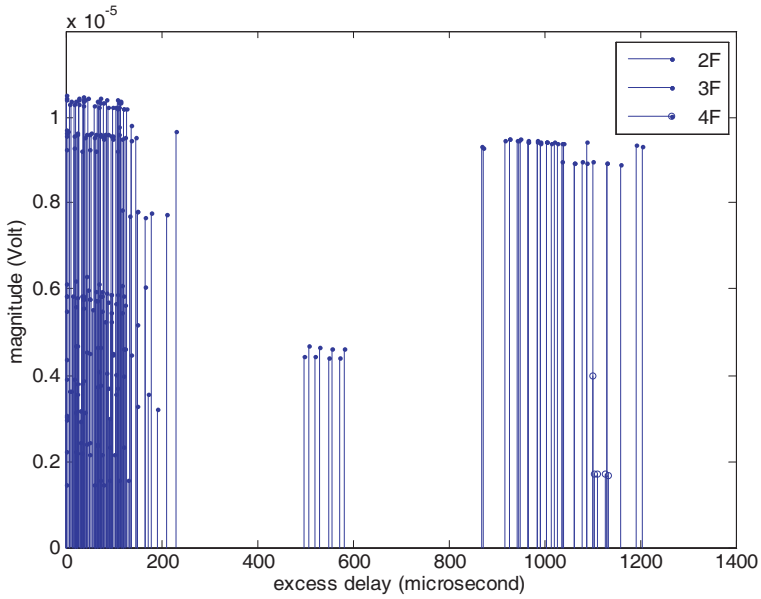

Figure 5. Received signal magnitudes with respect to excess delay for all paths from ray tracing.

3.3. Maximum Excess Delay

Based on the results of ray tracing, PDPs can be classified into two, i.e., those having paths originating from two modes and those with a single mode. The two modes referred here are mainly 2F and 3F, except for one PDP on September 11 at 07:00 LT containing paths in 3F and 4F. The maximum excess delays of PDPs consisting of two modes are longer than those from single mode PDPs. For example, on May 11 at 14:00 LT, the PDP consists of two modes, 2F and 3F, with maximum excess delay of 0.483 ms, while on September 11, 2015, the received path originates from one mode with shorter

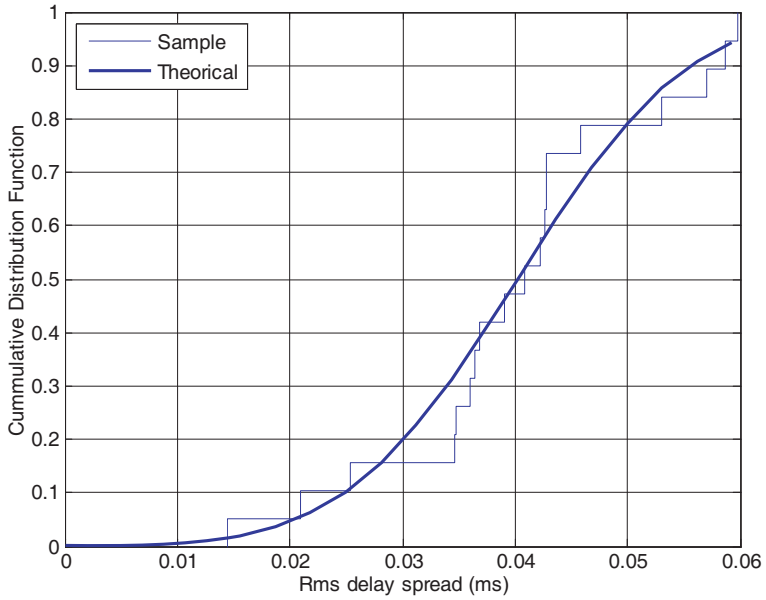

Figure 6. CDF of the rms delay spread from the result of ray tracing.

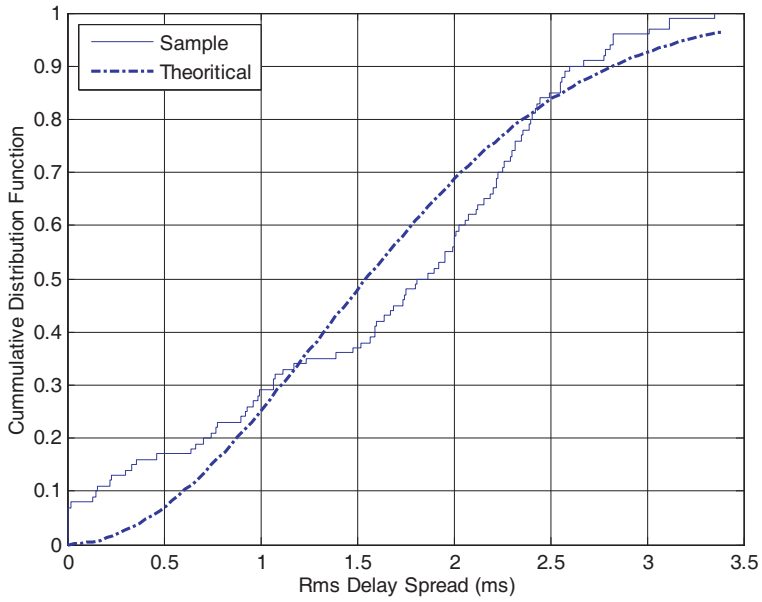

Figure 7. CDF of the rms delay spread from the Surabaya-Merauke measurement result on February 12–15, 2014.

maximum excess delay of 0.174 ms. Figure 8 depicts CDF of maximum excess delay for paths from a single mode, consisting of 20 samples.

K-S test suggests that maximum excess delay from ray tracing agrees with Gaussian distribution with mean 0.12 ms and standard deviation 0.043 ms. Similarly, as shown in Figure 9 and K-S tested, the measured maximum excess delay also approaches Gaussian distribution with mean 4.5138 ms and standard deviation 2.4321 ms. The difference in mean and variance is due to the presence of a single mode in the simulated channel and of multiple different modes in the measured channels. These two findings verify our hypothesis in Section 2.

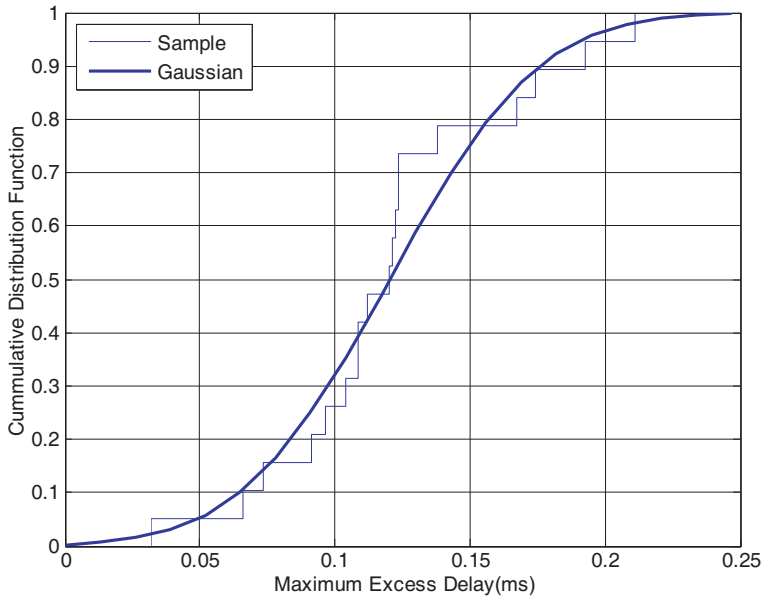

Figure 8. CDF of maximum excess delay from ray tracing result.

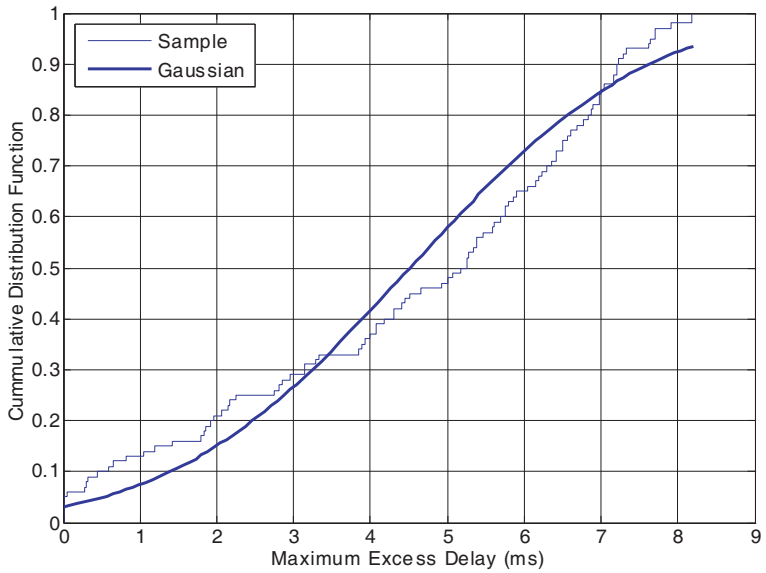

Figure 9. CDF of maximum excess delay from measurement on February 12–15, 2014.

4. CONCLUSION

We have shown a statistical model of wideband HF radio channel impulse response in a low-latitude region evaluated by ray-tracing simulation and real measurement on a 3044 km link. The results of simulation indicate that the channel gain is Rayleigh distributed, and path phase shift is uniformly distributed. It is found that the paths composing a channel impulse response are clustered following their propagation modes, which contradicts previous research [10] which states that the time delay for each path is randomly Gaussian. Results of grouping path elevation angles into delay bins can be used to choose an antenna with the desired elevation pattern to limit the modes arriving at the receiver, thereby alleviating inter-symbol interference. Rayleigh and Gaussian distributions are found to fit well rms delay spread and maximum excess delay, respectively.

Overall, the proposed statistical model describes the HF sky-wave long-distance channel impulse response behavior with multiple propagation modes. The model can be used in evaluation of HF long-distance communication systems in low latitudes.

ACKNOWLEDGMENT

This reported study was financially supported by Indonesian Ministry of Research, Technology and Higher Education through BPPDN scholarship to the first author and PUPT research grants, as well as PREDICT 2 grant from JICA Japan.

REFERENCES

1. Australian Government Bureau of Meteorology, *Introduction to HF Radio Propagation*, [Online], Available: www.sws.bom.gov.au/Educational/5/2/2, 2016.
2. McNamara, L., *The Ionosphere: Communications, Surveillance and Direction Finding*, Krieger, Florida, 1991.
3. Watterson, C. C., J. R. Juroshek, and W. D. Bensema, "Experimental confirmation of an HF channel model," *IEEE Trans. on Communication Technology*, Vol. 18, No. 6,792, 1970.
4. Mastrangelo, J. F., J. J. Lemmon, et al., "A new wideband high frequency channel simulation system," *IEEE Trans. on Communications*, Vol. 45, No. 1, 26, 1997.
5. Perry, B. and R. Rifkin, "Measured wideband HF mid latitude channel characteristic," *IEEE Military Communication Conference*, Boston, 1989.
6. Clune, M. and P. Fine, "Delay and doppler spreading characteristics of the wide-bandwidth HF channel," *Fifth International Conf. on HF Radio Systems and Technique*, Edinburg, 1991.
7. Yan, Z., L. Zhang, T. Rahman, and D. Su, "Prediction of the HF ionospheric channel stability based on the modified ITS model," *IEEE Trans. on Antenna and Propagation*, Vol. 16, No. 6, 3321, 2013.
8. Cannon, P. and M. J. Angling, "Measurements of the HF channel scattering function over Thailand," *Proc. International Antenna and Propagation Conf.*, Davos, 2000.
9. Rappaport, T., *Wireless Communications*, 160, Prentice-Hall, New York, 2002.
10. Lacaze, B., "Modeling the HF channel with Gaussian random delays," *Signal Processing*, Vol. 64, 215, 1997.
11. Solar Terestrial Dispatch, Proplab-Pro Version 3, 2010.
12. Mitran, R. and M. Stanic, "Delay spread evaluation of HF channels based on ray tracing," *2016 IEEE International Black Sea Conf. on Communication and Networking (BlackSeaComm)*, Varna, 2016.
13. Australian Government Beaureu of Meteorology, *Monthly Sunspot Number*, [Online], Available: www.sws.bom.gov.au/Solar/1/6.
14. Jones, R. and J. Stephenson, *Versatile Three Dimensional Ray Tracing Computer Program for Radio Wave in the Ionosphere*, US Gov. Printing Office, Washington D.C., 1975.
15. Williams, E., *Aviation Formulary V1.43*, [Online] Available: williams.best.vwh.net/avform.html, 2007.
16. Kurniawati, I., P. H. Mukti, R. Corputty, and G. Hendrantoro, "Preliminary study on HF channel complex impulse response and power delay," *XXXI URSI General Assembly and Scientific Symposium*, Beijing, 2014.
17. International Telecommunication Union, *Radio Regulations Articles*, ITU, 2016.
18. Sousa, E., V. Jovanovic, and C. Daigneault, "Delay spread measurement for the digital cellular channel," *IEEE Trans. on Vehicular Technology*, Vol. 43, No. 4, 837, 1994.
19. Hashemi, H., "Impulse response modelling of indoor radio propagation channels," *IEEE Journal on Selected Areas in Communications*, Vol. 11, No. 7, 967, 1993.
20. Dixon, W. J., J. Frank, and J. Massey, *Introduction to Statistical Analysis*, McGraw-Hill, New York, 1957.